Corrected copy

UNITED STATES
DEPARTMENT OF THE INTERIOR
GEOLOGICAL SURVEY

TECHNICAL LETTER NO. 1

THE PARKFIELD-CHOLAME, CALIFORNIA, EARTHQUAKES OF JUNE-AUGUST, 1966:

INSTRUMENTAL SEISMIC STUDIES

By Jerry P. Eaton

DENVER, COLORADO

This page intentionally left blank

UNITED STATES
DEPARTMENT OF THE INTERIOR
GEOLOGICAL SURVEY
National Center for Earthquake Research
345 Middlefield Road
Menlo Park, California, 94025

Technical Letter
NCER-1
February 1967

This Technical Letter--

TECHNICAL LETTER NO. 1

THE PARKFIELD-CHOLAME, CALIFORNIA, EARTHQUAKES OF JUNE-AUGUST, 1966:

INSTRUMENTAL SEISMIC STUDIES

By Jerry P. Eaton

--has been placed in the Open Files of the U. S. Geological Survey, and is publicly available in Geological Survey Libraries in Washington, D. C., Denver, Colorado, and Menlo Park, California. It will be published in the near future as one of a series of chapters in U. S. Geological Survey Professional Paper 579, "The Parkfield-Cholame, California, Earthquakes of June-August, 1966." Other chapters will discuss surface geologic, engineering, and water-resources aspects.

L. C. Pakiser

L. C. Pakiser
National Center for Earthquake Research

This page intentionally left blank

INSTRUMENTAL SEISMIC STUDIES

by

Jerry P. Eaton
U. S. Geological Survey, Menlo Park, California

INTRODUCTION

U. S. Geological Survey instrumental seismic studies in the Parkfield-Cholame area consist of three related parts that were undertaken as pilot studies in a program designed to develop improved tools and concepts for investigating the properties and behavior of the San Andreas fault. These studies include:

1. The long-term monitoring of the seismic background on the San Andreas fault in Cholame Valley by means of a short-period Benioff seismograph station at Gold Hill.

2. The investigation of the geometry of the zone of aftershocks of the June 27 earthquakes by means of a small portable cluster of short-period, primarily vertical-component, seismographs.

3. The seismic-refraction calibration of the region enclosing the aftershock source by means of three short reversed refraction profiles and a "calibration shot" near the epicenter of the main June 27 earthquake.

This brief report outlines the work that has been completed and presents some preliminary results obtained from analysis of records from Gold Hill and the portable cluster.

RESULTS FROM THE GOLD HILL SEISMOGRAPH

With support from the Advanced Research Projects Agency, Department of Defense, a Long Range Seismic Measurements "van" was installed at Gold Hill during October 1965, to record seismic waves from an underground nuclear explosion on Amchitka Island (the "Longshot" experiment). Gold Hill, a sliver of crystalline rock in the San Andreas rift zone on the northeast side of Cholame Valley (fig. 1) was suggested as a seismograph site by J. G. Vedder. This site was selected because it promised to be a quiet one, it filled a gap between the two California local earthquake networks (University of California at Berkeley in the north, and California Institute of Technology in the south), and it permitted the monitoring of small earthquakes on the San Andreas in a region where U. S. Geological Survey geologists were undertaking detailed studies of geologically recent movements along the fault.

For reasons of economy, only the 3-component short-period Benioff seismograph system was installed. When the 35-mm film records from all three components are enlarged 15 times in the film viewer, they provide ground displacement magnifications of about 200,000, and more than 600,000 (peak magnification) for waves with frequencies of 1 cps and 3 cps, respectively. The vertical component is also recorded at 1 mm/sec on a "Helicorder" monitor with ground displacement magnifications of about 75,000 and 240,000 (peak magnification) for waves with frequencies of 1 cps and 3 cps, respectively.

The Gold Hill records of the June 27 earthquakes and their aftershocks are of particular interest for a number of reasons:

1. Gold Hill was the nearest seismograph to the epicentral tract and augmented the Berkeley network so as to surround the epicenter of the main shock--Gold Hill data on the foreshocks, the main shock, and the principal aftershocks have already been utilized in Berkeley's epicenter determinations.

2. The surface faulting associated with the earthquakes followed the western flank of Gold Hill within 1,500 feet of the seismometer pits.

3. Continuous records of background seismic activity along the future fault break were obtained for a period of 8 months prior to rupture; and the foreshocks, the main shock, and all of the aftershocks were recorded by the same instruments at the same gain levels.

4. By the very-low-sensitivity direct seismic response of the radio-time-trace galvanometer and by the inertial offset of the film recorder drum (also visible as an offset in the radio time trace), the onset of varying levels of very strong motion at the Gold Hill van, 500 feet from the surface fault trace, can be detected and timed.

PRE-EARTHQUAKE SEISMIC ACTIVITY

The level of local seismic activity at Gold Hill from November 1965 through June 26, 1966, was extremely low--only 52 events with S-P intervals less than 4 seconds (epicentral distances less than about 30 km) were detected during the entire 34-week interval. Monthly totals were November, 8; December, 1; January, 6; February, 4; March, 1; April, 18; May, 11; and June, 3. Although these figures represented a considerable increase over previous months, the modest April and May totals did not single out the Parkfield-Cholame region for special attention prior to June 27.

RELATIONSHIPS AMONG FORESHOCKS, MAIN SHOCK, AND AFTERSHOCKS

Examination of the Gold Hill records and comparison of P arrival times at that station with those at Priest, the Berkeley station just east of the San Andreas fault 44.3 km northwest of Gold Hill, clearly indicate that the largest earthquake of the sequence, magnitude 5.5 at 04:26 on June 28 (Greenwich), was the one that accompanied breakage (or at least sudden movement) along the fault past Gold Hill. The first foreshock, of magnitude 3.1, was recorded at Gold Hill at 01:00:35.6 Z (June 28), 1.3 seconds earlier than at Priest. It was followed at 01:14:59.2 Z by a much smaller shock that recorded 0.8 seconds earlier at Gold Hill than at Priest. The third event of the sequence was the largest foreshock, with a magnitude of 5.1; it was recorded at Gold Hill at 04:09:00.4 Z, 1.2 seconds earlier than at Priest. The sole aftershock of this quake that was detected at Gold Hill was recorded at 04:18:38.2 Z, 1.1 seconds earlier than at Priest. Its magnitude was 2.6. The main earthquake, with a magnitude of 5.5, was recorded at Gold Hill at 04:26:17.4 Z, 1.6 seconds earlier than at Priest.

The instrumental epicenters of all of these earthquakes lie near the San Andreas fault northwest of Parkfield, at least 17 km northwest of Gold Hill. During the interval between the largest foreshock, whose magnitude approached that of the main shock, at 04:09 and the main shock at 04:26, no aftershock sequence was observable. When the Gold Hill trace quieted down so that it could be seen 9 minutes after the 04:26 earthquake, however, a strong aftershock sequence was in progress. During the first hour about four aftershocks per minute could be identified on the vertical component short-period Benioff film record. The first of these for which P could be timed arrived at Gold Hill 6.3 seconds earlier than at Priest. The frequency of aftershocks declined gradually from its maximum; and differences in P arrival times (Priest-Gold Hill) ranged from 0.8 second to more than 7 seconds, indicating that the aftershocks were originating all along the zone from somewhat northwest of the epicenter of the main shock to at least as far south-eastward as Gold Hill. Aftershocks with S-P intervals smaller than 1 second occurred throughout the sequence beginning with the main shock at 04:26. Thus, the aftershock sequence began at the time of the main shock, and the essential characteristics of the sequence that are indicative of the spatial distribution of individual aftershocks in relation to Gold Hill were established at the same time.

Assuming that the main earthquake, together with its foreshocks and aftershocks, occurred on the San Andreas fault between Gold Hill and Priest at a depth not greater than a few kilometers, we can use differences in P arrival times at Gold Hill and Priest to determine the approximate location of each quake. For such earthquakes the distance from Gold Hill to the epicenter is approximately ℓ (km) = 22.2 - 3 δ T, where a crustal P-wave speed of 6 km/sec has been assumed and δ T is the arrival time of P at Priest minus that at Gold Hill. Systematic errors in this simplified epicenter determination procedure result in calculated values for ℓ that are somewhat too large for most earthquakes, especially for earthquakes that originate near Gold Hill. Data required for calculating ℓ , and values of ℓ , for all of the foreshocks, the main earthquake, and the principal aftershocks recorded during the first 2 hours of the swarm are presented in table 1. The restriction of the epicenters of the foreshocks and the main earthquake to a small portion of the fault between 17 and 20 km northwest of Gold Hill and the scatter of aftershock epicenters along the fault from that region to at least as far southeastward as Gold Hill are clearly indicated. Similar data on a calibration shot located near the fault 21.4 km (the calculated value of ℓ is 20.4 km) northwest of Gold Hill are also presented in table 1.

Table 1.--Comparison of Gold Hill and Priest P-wave arrival time, 6/28/66 (Greenwich)

P arrival times Gold Hill	GH-Priest[1/] (sec)	Distance (km)	Magnitude[1/]
01-00-35.6	+1.3	18.3	3.1
01-14-59.2	+0.8	19.8	---
04-09-00.4	+1.2	18.6	5.1
04-18-38.2	+1.1	18.9	2.6
04-26-17.4 -3.4/ 14.0	+1.6	17.4	5.5
04-35-00.8	+6.3	3.3	3.0
04-42-35.2	+6.8	1.8	1.9
05-01-01.2	+6.0	4.2	3.1
05-03-47.3	+4.2	9.6	1.9
05-09-54.4	[2/] +7.7	----	2.0
05-12-45.6	+3.1	12.9	2.4
05-29-18.2	+2.9	13.5	1.6
05-37-06.6	+5.2	6.6	2.0
05-40-23.1	+2.2	15.6	2.2
06-32-22.0	+1.5	17.7	3.4
06-35-13.2	+6.7	2.1	2.5
06-39-33.9	+3.9	10.5	1.7
07-33-55.4	+3.9	10.5	2.2
Calibration Shot 9/15/66 (Greenwich)			
12-00-05.0	+0.6	20.4	2600# charge

[1/] Magnitudes and Priest arrival times were provided by Prof. T. V. McEvilly, University of California at Berkeley.

[2/] Epicenter is SE of Gold Hill and cannot be determined by this technique.

FREQUENCY OF AFTERSHOCKS

To provide uniform treatment of the entire aftershock sequence, an attempt was made to count all discernible aftershocks on the Helicorder monitor of the vertical-component Benioff seismograph at Gold Hill. Starting 12 hours after the main shock, this task was relatively simple--total aftershock counts were made directly on the monitor for each record interval (usually about 24 hours), and the average rate of occurrence of aftershocks during each interval was computed. The power supply for the Helicorder was out of operation for several hours after the main shock; so hourly totals of aftershocks were determined from the film record of the vertical-component Benioff seismograph for the first 12 hours. The rate of occurrence of aftershocks determined from the film record for each of these hourly intervals was adjusted to that expected on the Helicorder by comparing the total number of events on the two records between 07:55 Z and 16:25 Z, June 28, when both recorders were in operation.

Figure 1 and table 2 show the frequency of aftershocks as a function of time as recorded at Gold Hill.

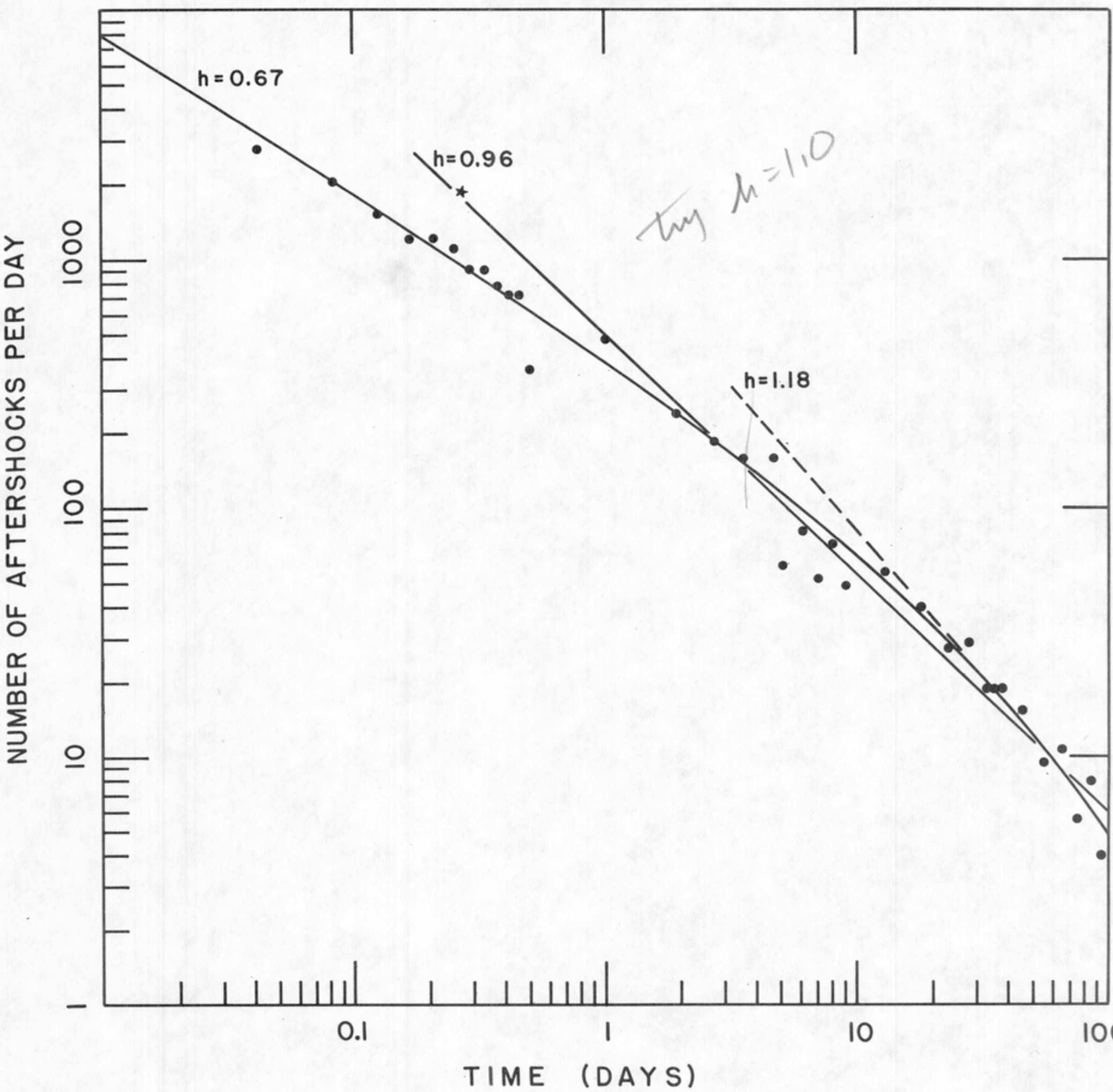

Figure 1.--Frequency of aftershocks at Gold Hill as a function of time for 96 days after the main shock. Solid circles represent hourly averages for the first 12 hours, daily averages for the next 5 days, 5-day averages for the next 30 days, and 10-day averages thereafter. The star represents events during the first 12 hours when they are lumped into a single interval. The h's refer to the rate of decay of the aftershock sequence according to the empirical equation $R(t)= R_o t^{-h}$.

Table 2.--Frequency of aftershocks recorded at Gold Hill

Interval	Rate (quakes/day)	
June 28, 05:00 to 06:00	2,760	1,186/day 05:00 to 17:00 (05:00 to 17:00 group)
06:00 to 07:00	2,064	
07:00 to 08:00	1,511	
08:00 to 09:00	1,200	
09:00 to 10:00	1,224	
10:00 to 11:00	1,104	
11:00 to 12:00	912	
12:00 to 13:00	912	
13:00 to 14:00	774	
14:00 to 15:00	720	
15:00 to 16:00	720	
16:00 to 17:00	360	
June 28, 17:00 to June 29, 16:00	480	
June 29, 16:00 to June 30, 12:00	241	
June 30, 12:00 to July 1, 05:00	186	
July 1, 05:00 to July 2, 04:00	160	
July 2, 04:00 to July 2, 17:00	159	
July 2, 17:00 to July 3, 18:00	59	
July 3, 18:00 to July 4, 16:00	81	
July 4, 16:00 to July 5, 16:00	52	
July 5, 16:00 to July 6, 17:00	72	

Table 2.--Frequency of aftershocks recorded at Gold Hill (continued)

Interval	Rate (quakes/day)
July 6, 17:00 to July 7, 17:00	49
July 7, 17:00 to July 8, 22:00	45
July 8, 22:00 to July 14, 01:00	56
July 14, 01:00 to July 19, 00:00	40
July 19, 00:00 to July 24, 00:00	25
July 24, 00:00 to July 28, 15:00	27
July 28, 15:00 to Aug. 2, 16:00	19
Aug. 2, 16:00 to Aug. 7, 14:00	19
Aug. 7, 14:00 to Aug. 17, 12:00	16
Aug. 17, 12:00 to Aug. 27, 13:00	10
Aug. 27, 13:00 to Sept. 6, 16:00	11
Sept. 6, 16:00 to Sept. 16, 19:00	6
Sept. 16, 19:00 to Sept. 26, 16:00	8
Sept. 26, 16:00 to Oct. 2, 16:00	4

Investigators in Japan (Mogi, 1962) have found that the frequency of aftershocks as a function of time, for a number of Japanese earthquakes, can be adequately represented by a pair of empirical relationships:

$$R(t) = R_o t^{-h}, \quad 0 < t < 100 \text{ days};$$

$$R(t) = N_o e^{-pt}, \quad t > 100 \text{ days};$$

where R(t) is the frequency of aftershocks at time t after the main shock and Ro, No, h, and p are constants. The first equation implies a linear relationship between log R and log t; the second, between log R and t. On a plot of log R vs log t, data from the first 100 days of the aftershock sequences of the Tottori (1943) and Tokachi (1952) earthquakes are adequately fit by straight lines with h equal to 1:36 and 0.98, respectively (Mogi, 1962).

A similar plot of data for the Parkfield-Cholame earthquake (fig. 1) appears to be best fit by a curve that deflects downward with respect to a straight line as time increases. Tangents to this curve which fit the plotted points from 0 to 4+ days and from 10 to 96 days have h equal to 0.67 and 1.18, respectively. The apparent differences between this case and those reported by Mogi may result from differences in the time intervals over which aftershocks were counted for the purpose of determining the aftershock frequencies. For example, if aftershocks during the first 12 hours of the Parkfield-Cholame sequence were added together and plotted at t = 0.27 day (asterisk on fig. 1), it would be possible to fit all of the data fairly well with a straight line with h = 0.96.

Possibly a better method of displaying aftershock sequences would be to plot curves showing cumulative total aftershock counts as a function of time. Necessary smoothing of the raw data could be accomplished in the process of abstracting information from the seismograms, for example, by recording the times at which the cumulative total of aftershocks reached prescribed values such as 100, 200, 300, etc. Frequency curves would be calculated readily from such a set of cumulative total vs time number pairs.

It appears, however, that the progressive increase in the rate of decay of the Parkfield-Cholame aftershock sequence is real--at least, there is a clear difference before and after t = 10 days. This phenomenon may be related to the relatively large amount of post-earthquake creep along the surface that slipped suddenly at the time of the main shock; the "sudden" redistribution of stress in the vicinity of the fault, usually held to be responsible for aftershock sequences, was effectively prolonged after the time of initial rupture by creep along the fault. In this view, the later portion of the frequency vs time curve is tending toward a normal slope, and the early part is abnormal.

RECORD OF INTENSE GROUND MOTION

With the arrival of P waves from the main shock at 04:26:17.4, all regular seismic traces at Gold Hill were "blanked out" for nearly 10 minutes. The fourth channel on the 35-mm film recorder, which normally records the rectified audio signal from WWV to provide frequent chronometer corrections, responded to the intense motion of the ground at the recording site and wrote an interpretable record of it. Abnormal deflections of the radio trace appear to have resulted both from the direct seismic response of the recording galvanometer and from axial excursions of the recording drum, which is normally restrained by a friction clamp.

Immediately prior to the quake the radio trace was recording a slowly varying audio WWV "tone" punctuated by the 40-millisecond interruptions that mark individual seconds. These "second ticks" can be seen clearly on figure 2, a sketch of the critical portion of the record, before and during the first few seconds of the earthquake. The actual times of several of the second marks are indicated on the sketch, where an irregular advance of the drum during the earthquake is evidenced by the uneven spacing of the second marks. The arrival of the P waves is marked by a slight widening of the trace at 04:26:17.4; and a moderate increase in shaking occurred about 1 second later. Still stronger longer-period motion (possibly S) began just before 04:26:21. At about 04:26:22 the inertial forces acting on the drum overcame its frictional restraints, and the ground and recorder carriage moved to and fro beneath the drum for about 6 seconds. The slipping of the drum on the shaft was overcome by the friction clamp at about 04:26:28. For the next 20 seconds, a decaying train of waves with a period of about 1/2 second was recorded. Because the radio power was shut off when commercial power to the van was interrupted during the strong shaking, radio time marks are absent after 04:26:28.

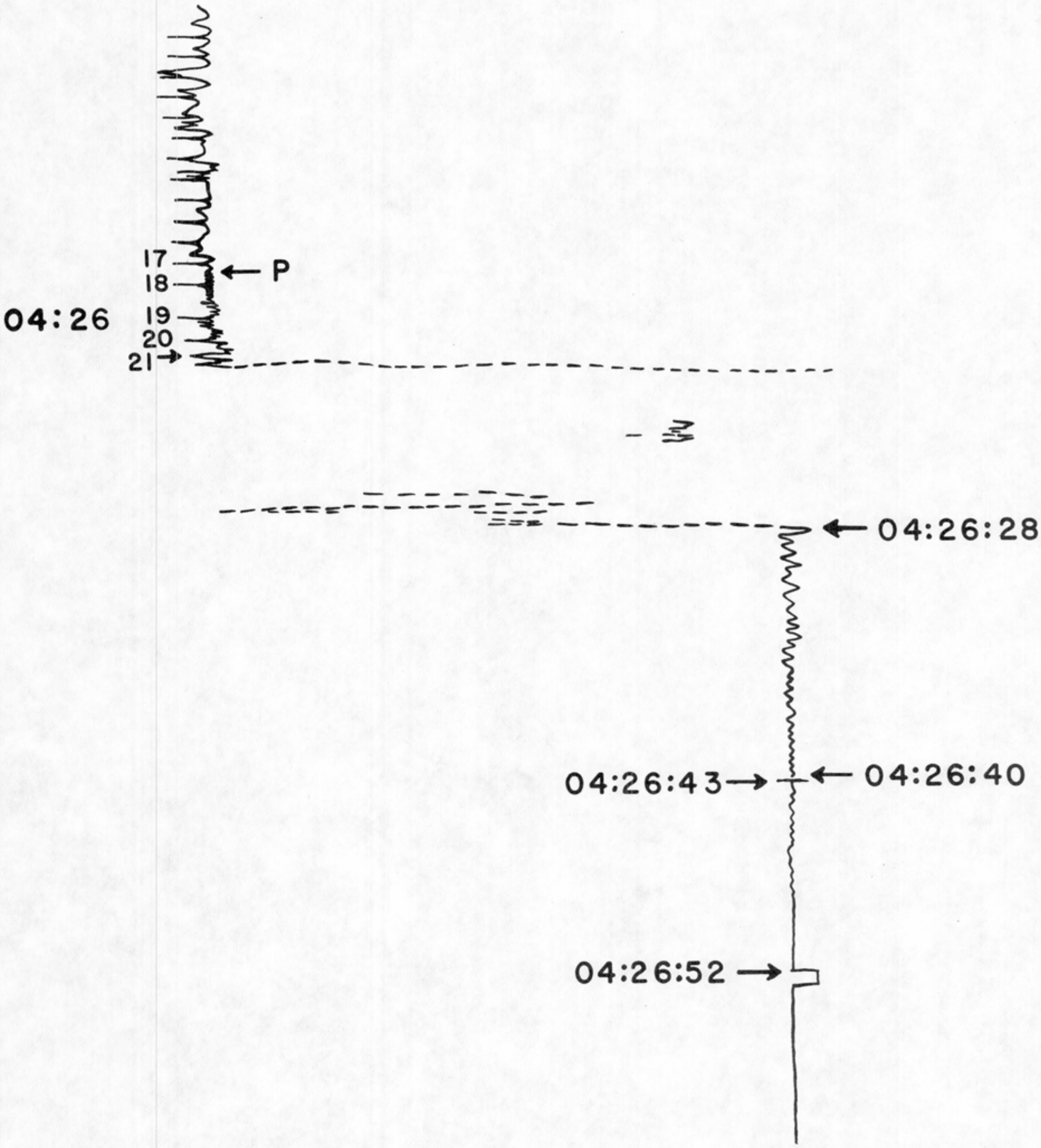

Figure 2.--Abnormal behavior of the radio time trace on the 35 mm film recorder produced by strong ground motion at the Gold Hill van. Indicated times are Greenwich. Dotted lines indicate very faint portions of the trace that were written while the drum was sliding to and fro on its shaft.

The event, possibly related to the propagating end of the ruptured zone on the fault, that reached Gold Hill at 04:26:22 and caused the recording drum to slip on its shaft traveled from the focus at an average speed of 2.2 km/sec. This speed is significantly lower than that (3.3 to 3.5 km/sec) appropriate for S waves traveling through the upper part of the crystalline crust. The duration of shaking that was sufficiently intense to keep the drum in motion against its frictional restraints was only 6 seconds.

GEOMETRY OF THE AFTERSHOCK SOURCE REGION SOUTHEAST OF GOLD HILL

To study the relationship between the surface fault break and the aftershocks of the Parkfield-Cholame earthquake, a small cluster of portable seismographs was laid out around the portion of the surface break that lies southeast of Gold Hill. Locations and periods of operation of individual stations are listed in table 3. The basic cluster consisted of Gold Hill and eight portable stations in a 20-km-diameter pattern with five stations along the fault and two pairs of stations about 10 km from the fault on either side of it (fig. 3). During the last two weeks of the experiment, four additional portable stations were laid out to extend coverage northwestward along the fault (stations 9, 10, 12, and 13), and another was installed at Gold Hill to supplement the Benioff seismograph. At most stations, only a vertical-component seismograph was operated.

Table 3.--U. S. Geological Survey seismograph stations in the Parkfield-Cholame area

Station	Lat, N	Long, W	Ht. (feet)	Installed	Removed
Gold Hill	35° 49.88'	120° 21.18'	1430	Oct '65	-------
1	" 45.30'	" 18.70'	1220	6/30/66	9/15/66
2	" 47.36'	" 21.44'	1240	6/30/66	9/16/66
3	" 43.20'	" 16.85'	1370	6/30/66	9/15/66
4	" 48.82'	" 16.07'	1590	6/30/66	9/15/66
5	" 42.61'	" 22.72'	1470	6/30/66	9/15/66
6	" 40.30'	" 12.65'	2100	6/30/66	9/15/66
7	" 39.06'	" 19.22'	1530	7/9/66	9/15/66
8a	" 47.23'	" 11.06'	1615	7/9/66	8/14/66
8b	" 47.39'	" 10.55'	1700	8/14/66	9/15/66
9	" 52.79'	" 24.72'	1540	9/1/66	9/16/66
10	" 49.47'	" 26.41'	2120	9/2/66	9/16/66
11	" 49.88'	" 21.18'	1430	9/3/66	9/16/66
12	" 53.33'	" 20.55'	1800	9/5/66	9/16/66
13	" 55.09'	" 26.69'	1980	9/6/66	9/16/66

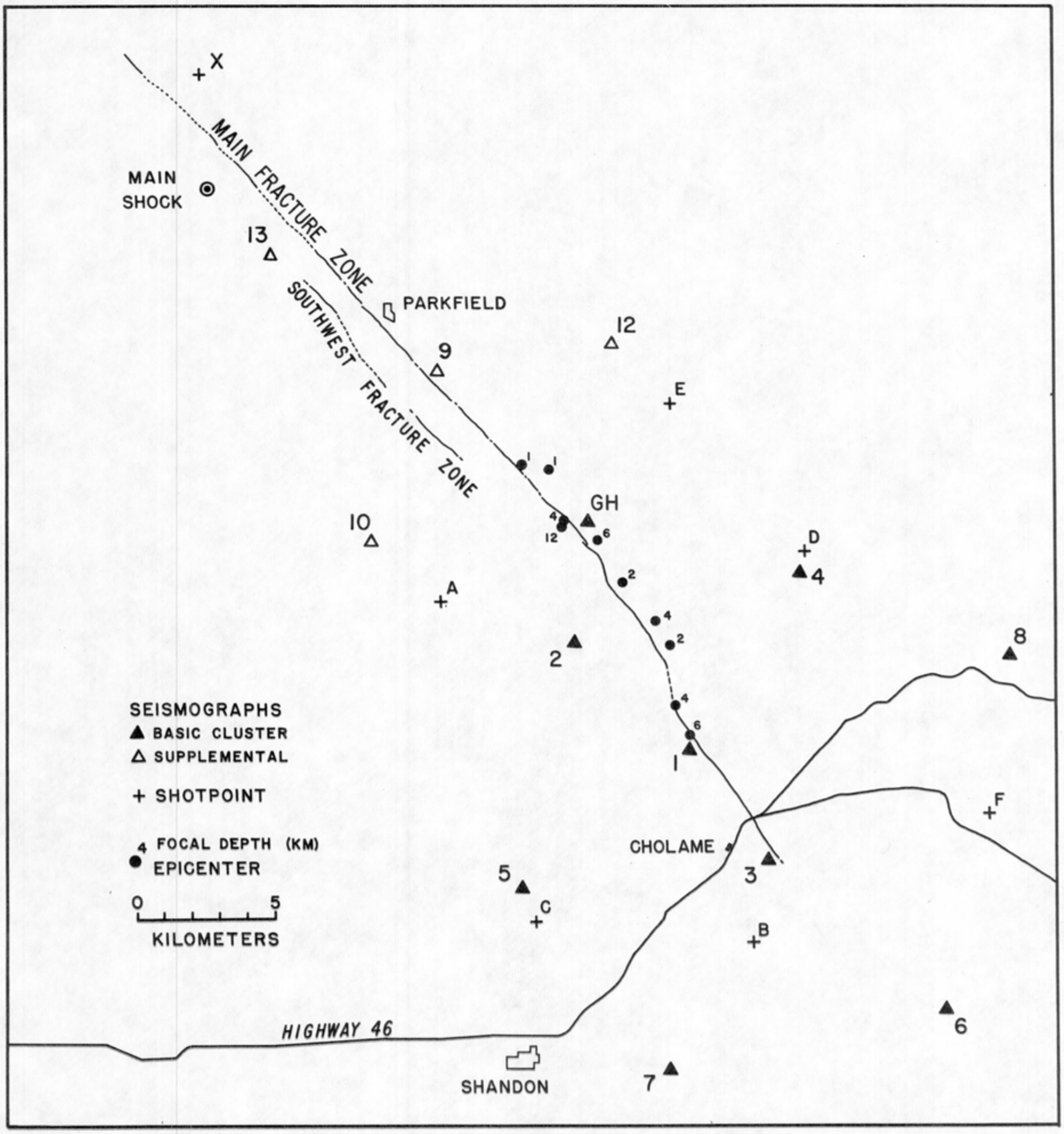

Figure 3.--Sketch map of the Parkfield-Cholame region showing U. S. Geological Survey seismograph stations, epicenters of July 17, 1966, aftershocks, refraction and calibration shot locations, and the surface fracture zones associated with the 1966 earthquake sequence (from a map by R. D. Brown and J. G. Vedder, U. S. Geological Survey). The epicenter of the main shock was provided by Prof. T. V. McEvilly, University of California at Berkeley.

Overall system response increased 6 db per octave with increasing frequency between the lower limit set by the 1-cps seismometer and the 17-cps upper limit set by the low-speed tape recorder. Amplifier gain levels were set so that the prevailing background noise produced about 10 percent modulation on the high-level tape channel. A second channel recorded with 30 db greater attenuation. Primary timing was provided by the continuous recording of WWVB, and a crystal chronometer supplemented WWVB during brief broadcast interruptions or receiver malfunctions. Events on the tape "playbacks" can be timed to within 0.01 second.

Complete analysis of data from the portable cluster will require some time; so a short time sample was analyzed in a preliminary effort to establish analytical procedures and to survey the kind and quality of results that can be obtained. All events discernible on the Gold Hill monitor record during the quiet hours of the night of July 16 and July 17 (about 04:00 Z to 13:00 Z on July 17) were played back for the other eight stations of the basic cluster. Of the 13 events selected in this manner (table 4), 3 lay so far northwest of the cluster that their foci could not be determined with accuracy, 2 lay only a few kilometers northwest of Gold Hill, and the remaining 8 lay very near or southeast of Gold Hill. This sample is not a uniform one of all events occurring throughout the aftershock source region because most of the small events of which it is composed would not have been detected at all if they had occurred near the northwest end of the zone of surface fracture.

Table 4.--Aftershocks detected at Gold Hill between 04:00 Z and 13:00 Z July 17

	Origin time	Depth (km)	Location Lat. N.	 Long. W.	Av $\lvert \varepsilon \rvert$ (sec)
1	05-55-00	------	NW of cluster		---
2	07-12-03.55	6	35° 49.5'	120° 20.9'	0.06
3	07-25-21.20	1±	" 51.0'	" 22.7'	.09
4	08-23-54.8	1±	" 50.9'	" 22.0'	---
5	08-43-46.37	6	" 45.7'	" 18.7'	.04
6	09-51-30.91	2	" 48.7'	" 20.3'	.04
7	10-19-41.32	4	" 49.9'	" 21.7'	.05
8	10-47-01.80	4	" 47.9'	" 19.5'	.07
9	10-50-31.85	12	" 49.8'	" 21.8'	.06
10	11-19-10.90	4	" 46.3'	" 19.0'	.06
11	12-19-29	------	NW of cluster		---
12	12-40-02	------	NW of cluster		---
13	12-46-35.5	1±	" 47.4'	" 19.2'	.06

To determine the foci of these aftershocks, a series of isochron charts constructed for quakes at various focal depths in a crustal model (fig. 4) established by refraction profiling between Camp Roberts (30 km west of Cholame) and San Francisco were used (Healy, 1963; Eaton, 1966). This method is based on that described by Riznichenko and others (Riznichenko, 1960). The epicenter and focal depths selected are those which yield the smallest P-wave arrival time residuals at available stations. For the events near or within the network, which were successfully located, average (absolute value) residuals ranged from 0.04 second to 0.09 second.

Epicenters and focal depths of the 10 "located" aftershocks in table 4 are indicated on figure 3. The epicenters lie very close to the trace of the main fracture zone, and there appears to be no sorting of earthquakes with respect to distance from the surface break as a function of focal depth. Thus, it appears that the aftershocks included in this small sample occurred on or very near a fault surface that extends vertically downward from the surface break to a depth of about 12 km.

To indicate the sensitivity of the cluster to variations in focal depth, P-wave travel-time curves for earthquakes at various depths between 2 km and 14 km are given in figure 5. Observed arrivals from four aftershocks with different focal depths are plotted on figure 5 for comparison. This comparison illustrates how the range in recording distance, and scatter in arrival times, of

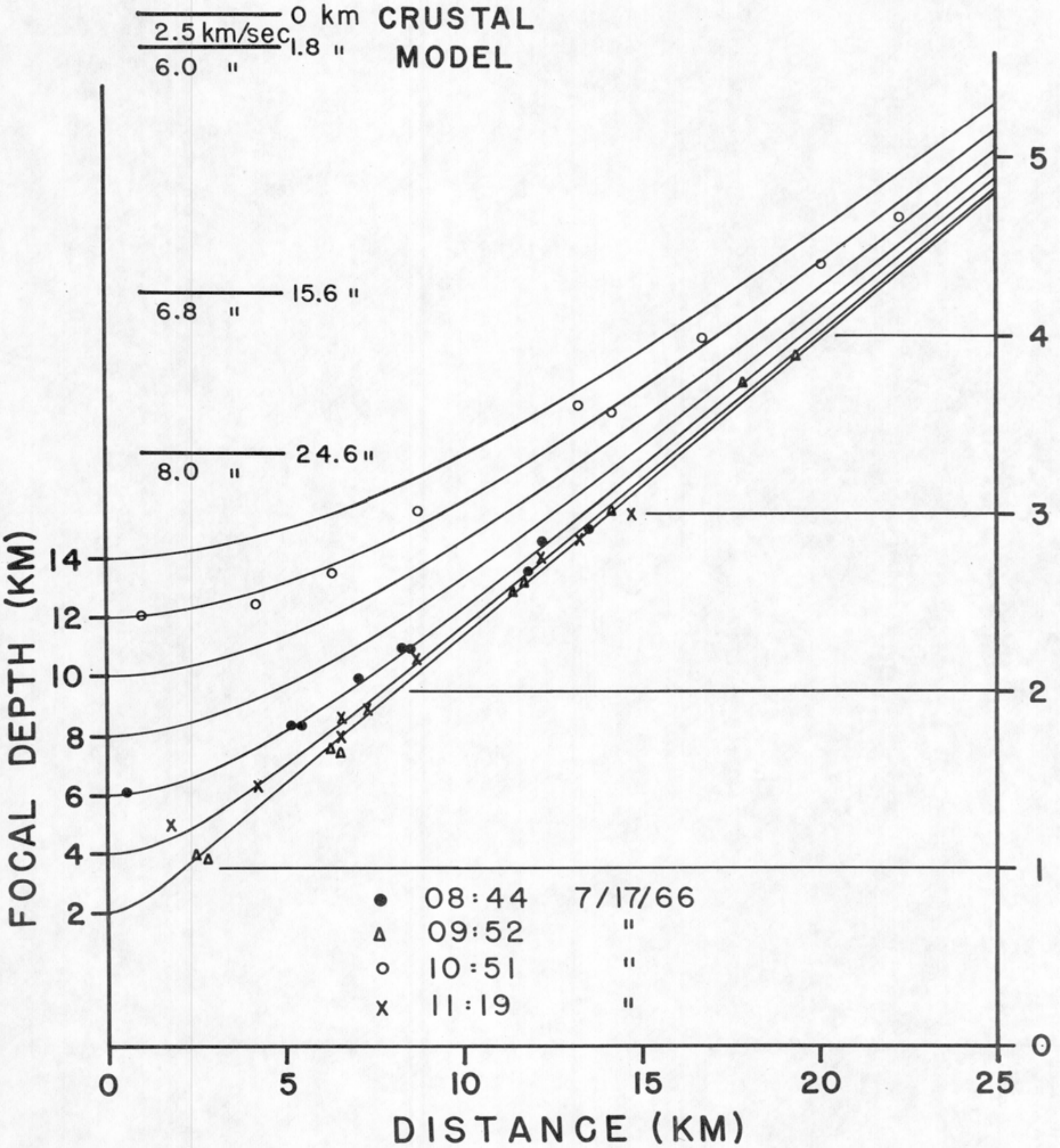

Figure 4.--Theoretical traveltime curves for earthquakes with focal depths from 2 to 14 km and the crustal model from which they were calculated. Observations from four July 17 aftershocks (table 4) are plotted on the diagram for comparison with the theoretical curves.

observations from individual earthquakes limit the precision with which focal depths can be determined. If ±1 km precision is sought, some observations at epicentral distances as small as the focal depth are required.

SEISMIC-REFRACTION CALIBRATION OF THE CRUST IN THE AFTERSHOCK REGION

To approach maximum precision in locating aftershocks in three dimensions, more detailed information on crustal structure beneath the cluster is required. This need is particularly acute when the cluster is cut by a geologic discontinuity as profound as the San Andreas fault.

On September 13, 14, and 15, eight explosive charges ranging in weight from 310 to 2,600 pounds were detonated in drill holes to provide sources for three 20-km-long reversed seismic-refraction profiles and one calibration shot to help refine the epicenter assigned to the major earthquake. Essential data on the shots are listed in table 5, and the shot points are plotted on figure 3. Nine mobile refraction units employing six vertical-component 1-cps seismometers at 1/2-km spacing and two horizontal-component 1-cps seismometers at one of the vertical locations, plus two shot-point units employing four vertical component 2-cps seismometers at 1/2-km spacing, were deployed along lines connecting pairs of shot points to record the refraction profiles. Profile A-B was designed to

Table 5.--USGS calibration shots in the Parkfield-Cholame area

Shot	Charge (lb)	Lat. (North)	Long. (West)	Height (feet)	Detonation	Time
A	540	35° 48.30'	120° 24.64'	2140	04:00:00.35	Sept. 13
B	540	" 41.61'	" 17.23'	1550	04:29:59.79	"
C	540	" 41.99'	" 22.41'	1380	03:59:59.00	Sept. 15
D_1	310	" 49.27'	" 15.98'	1660	05:59:59.86	Sept. 14
D_2	1,020	" 49.27'	" 15.97'	1660	04:30:00.28	Sept. 15
E	540	" 52.23'	" 19.28'	1640	03:59:59.82	Sept. 14
F	540	" 44.14	" 11.59'	1560	04:29:59.88	Sept. 14
X	2,600	" 58.64'	" 30.38'	2030	04:59:59.82	Sept. 15

determine near-surface and upper-crust properties on the southwest side of the fault; and profile E-F was designed for the same purpose on the northeast side of the fault. A transverse profile between C and D was recorded to test for possible velocity perturbations in the rift zone itself. The 2,600-pound calibration shot (X) was detonated at a convenient location a few kilometers north of the instrumental epicenter of the main earthquake. The mobile refraction equipment was laid out between C and D to record it.

Because all eight shots were recorded by the augmented cluster (Gold Hill plus portable stations at the 12 other sites), they should provide the data required for the calculation of individual station corrections that are needed for the further refinement of aftershock epicenters.

Work on the analysis of the refraction and calibration data is in progress.

REFERENCES CITED

Eaton, J. P., 1966, Crustal structure in northern and central California from seismic evidence in Geology of northern California, Calif. Div. of Mines and Geol. Bull. 190.

Healy, J. H., 1963, Crustal structure along the coast of California from seismic-refraction measurements: Jour. Geophysical Res., v. 68, no. 20, pp. 5777-5787.

Mogi, Kiyoo, 1962, On the time distribution of aftershocks accompanying the recent major earthquakes in and near Japan: Tokyo Univ. Earthquake Research Inst. Bull., v. 40, pt. 1, p. 107-124.